JCB Article

Trafficking of Lyn through the Golgi caveolin involves the charged residues on αE and αI helices in the kinase domain

Kousuke Kasahara, Yuji Nakayama, Kikuko Ikeda, Yuka Fukushima, Daisuke Matsuda, Shinya Horimoto, and Naoto Yamaguchi

Department of Molecular Cell Biology, Graduate School of Pharmaceutical Sciences, Chiba University, Chiba 260-8675, Japan

Src-family kinases, known to participate in signaling pathways of a variety of surface receptors, are localized to the cytoplasmic side of the plasma membrane through lipid modification. We show here that Lyn, a member of the Src-family kinases, is biosynthetically transported to the plasma membrane via the Golgi pool of caveolin along the secretory pathway. The trafficking of Lyn from the Golgi apparatus to the plasma membrane is inhibited by deletion of the kinase domain or Csk-induced "closed conformation" but not by kinase inactivation. Four residues (Asp346 and Glu353 on αE helix, and Asp498 and Asp499 on αI helix) present in the C-lobe of the kinase domain, which can be exposed to the molecular surface through an "open conformation," are identified as being involved in export of Lyn from the Golgi apparatus toward the plasma membrane but not targeting to the Golgi apparatus. Thus, the kinase domain of Lyn plays a role in Lyn trafficking besides catalysis of substrate phosphorylation.

Introduction

Src-family protein-tyrosine kinases, which belong to a family of nonreceptor-type tyrosine kinases, comprise proto-oncogene products and structurally related proteins, and include at least eight members with significant amino acid sequence homology (c-Src, Lyn, c-Yes, Fyn, c-Fgr, Hck, Lck, and Blk). Src-family kinases are known to play crucial roles in regulating proliferation and differentiation, especially cell growth control, gene expression, metabolism, and cytoskeletal architecture (Thomas and Brugge, 1997). Multiple combinations of Src-family kinase members are expressed in many cell types and are involved in individual and overlapping signaling pathways (Korade-Mirnics and Corey, 2000).

Src-family kinases are composed of: (a) an NH_2-terminal Src homology (SH) 4 domain that contains lipid modification sites for myristoylation mostly together with palmitoylation; (b) a poorly conserved "unique" domain, which is hypervariable among Src-family kinases; (c) an SH3 domain, which can bind to specific proline-rich sequences; (d) an SH2 domain, which can bind to specific sites of tyrosine phosphorylation; (e) an SH1 tyrosine kinase catalytic domain; and (f) a COOH-terminal negative regulatory tail for autoinhibition of kinase activity (Brown and Cooper, 1996). The tyrosine kinase activity of Src-family kinases is repressed through creating a distinctive "closed conformation" due to the intramolecular bindings of the SH2 domain to the tyrosine-phosphorylated tail catalyzed by the Csk-family and of the SH3 domain to the SH2-kinase linker (Sicheri et al., 1997; Xu et al., 1997). The absence of this COOH-terminal tyrosine residue, as found in the viral oncogenic forms, leads to cell transformation due to constitutive kinase-activation by derepression (Brown and Cooper, 1996; Blume-Jensen and Hunter, 2001).

Src-family kinases, classified as cytosolic enzymes, are localized at the cytoplasmic face of the plasma membrane through posttranslational myristoylation (Resh, 1994), but an appreciable fraction is found at the perinuclear region (Resh and Erikson, 1985; David-Pfeuty and Nouvian-Dooghe, 1990), which may correspond to associate with late endosomes (Kaplan et al., 1992), and at other locations including synaptic vesicles (Linstedt et al., 1992) and secretory granules/phagosomes (Mohn et al., 1995). Previous studies on c-Src, Lck,

Address correspondence to Naoto Yamaguchi, Dept. of Molecular Cell Biology, Graduate School of Pharmaceutical Sciences, Chiba University, Inohana 1-8-1, Chuo-ku, Chiba 260-8675, Japan. Tel./Fax: 81-43-226-2868. email: nyama@p.chiba-u.ac.jp

Key words: FRAP; intracellular localization; secretory pathway; open conformation; Src-family tyrosine kinase

Abbreviations used in this paper: BFA, brefeldin A; CHX, cycloheximide; GalT, β-1,4-galactosyltransferase; NEM, *N*-ethyl-maleimide; SH, Src homology.

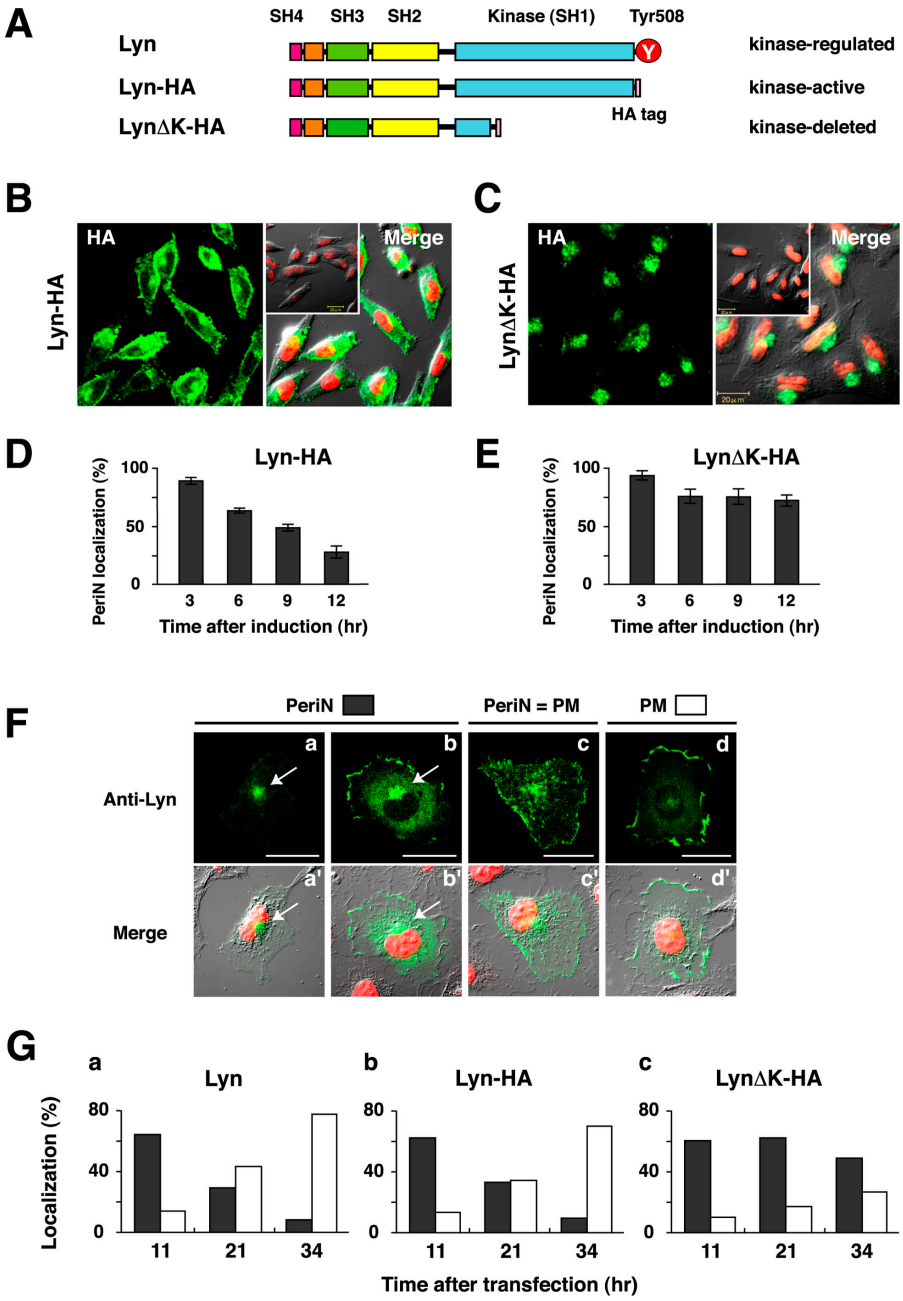

Figure 1. **Perinuclear localization of Lyn and its mutants.** (A) Schematic representations of Lyn and its mutants are shown with the Src homology (SH) domains, the negative-regulatory tyrosine (Y), and the HA-epitope tag. HeLa cells inducibly expressing Lyn-HA (B) or LynΔK-HA (C) were cultured in the absence (insets) or presence of 1 μg/ml doxycycline for 2 d, and stained with anti-HA. Lyn, green; DNA, red. Bars, 20 μm. HeLa cells inducibly expressing Lyn-HA (D) or LynΔK-HA (E) were cultured in the presence of 3 μg/ml doxycycline for the indicated periods, and stained with anti-HA. Cells exhibiting the perinuclear localization of Lyn as seen in C were quantified. Results (%) are the mean ± SD from three independent experiments. Protein expression was not detected until 3 h of induction. (F) COS-1 cells transfected with Lyn and its mutants were cultured for 24 h, stained with anti-Lyn. Three patterns of Lyn localization are shown: PeriN (a, a′, b, b′), PeriN = PM (c, c′), and PM (d, d′), as described in Materials and methods. Arrows indicate the perinuclear region. Bars, 20 μm. (G) A representative analysis of each Lyn mutant is shown. COS-1 cells transfected with Lyn (a), Lyn-HA (b), or LynΔK-HA (c) were cultured for the indicated periods. Lyn localization was quantified according to the classification as described in F. PeriN, filled bars; PM, open bars. Protein expression was not detected until 11 h after transfection.

Fyn, and Hck (David-Pfeuty and Nouvian-Dooghe, 1990; Kaplan et al., 1992; Ley et al., 1994; Gauen et al., 1996; Bijlmakers et al., 1997; van't Hof and Resh, 1997; Bijlmakers and Marsh, 1999; Carreno et al., 2000) elaborately explored the localizations of the Src-family kinases by immunostaining or pulse-radiolabeling and -chase experiments coupled with subcellular fractionation. Although distinctive localizations of individual members of Src-family kinases have been implicated in their specific functions, the mechanism of their diverse intracellular localizations has thus far not been fully provided. Therefore, we wished to examine how Src-family kinases can localize and to determine which elements can function for the localization.

Here, we chose Lyn that belongs to a member of the Src-family kinases because Lyn is widely expressed in a variety of organs, tissues, and cell types such as epidermoid, hematopoietic, and neuronal cells, and plays an important role in signal transduction at the cytoplasmic side of the plasma membrane (Tsukita et al., 1991; Radha et al., 1996; Healy and Goodnow, 1998; Hirao et al., 1998; Hayashi et al., 1999; Dykstra et al., 2001). To explore the basis that determines intracellular localization of Lyn, we took an approach for spatial and temporal detection of Lyn and its mutants, using an inducible or transient expression of Lyn or Lyn fused with the GFP visualized by confocal laser microscopy.

Here, we show that Lyn is mainly localized to both the plasma membrane and a fraction of caveolin, a marker for a class of endosomes, which is present at the Golgi apparatus. After biosynthesis, Lyn is rapidly associated with the Golgi pool of caveolin, and then transported to the plasma membrane. The trafficking of Lyn from the Golgi apparatus to the plasma membrane requires the kinase domain per se but not

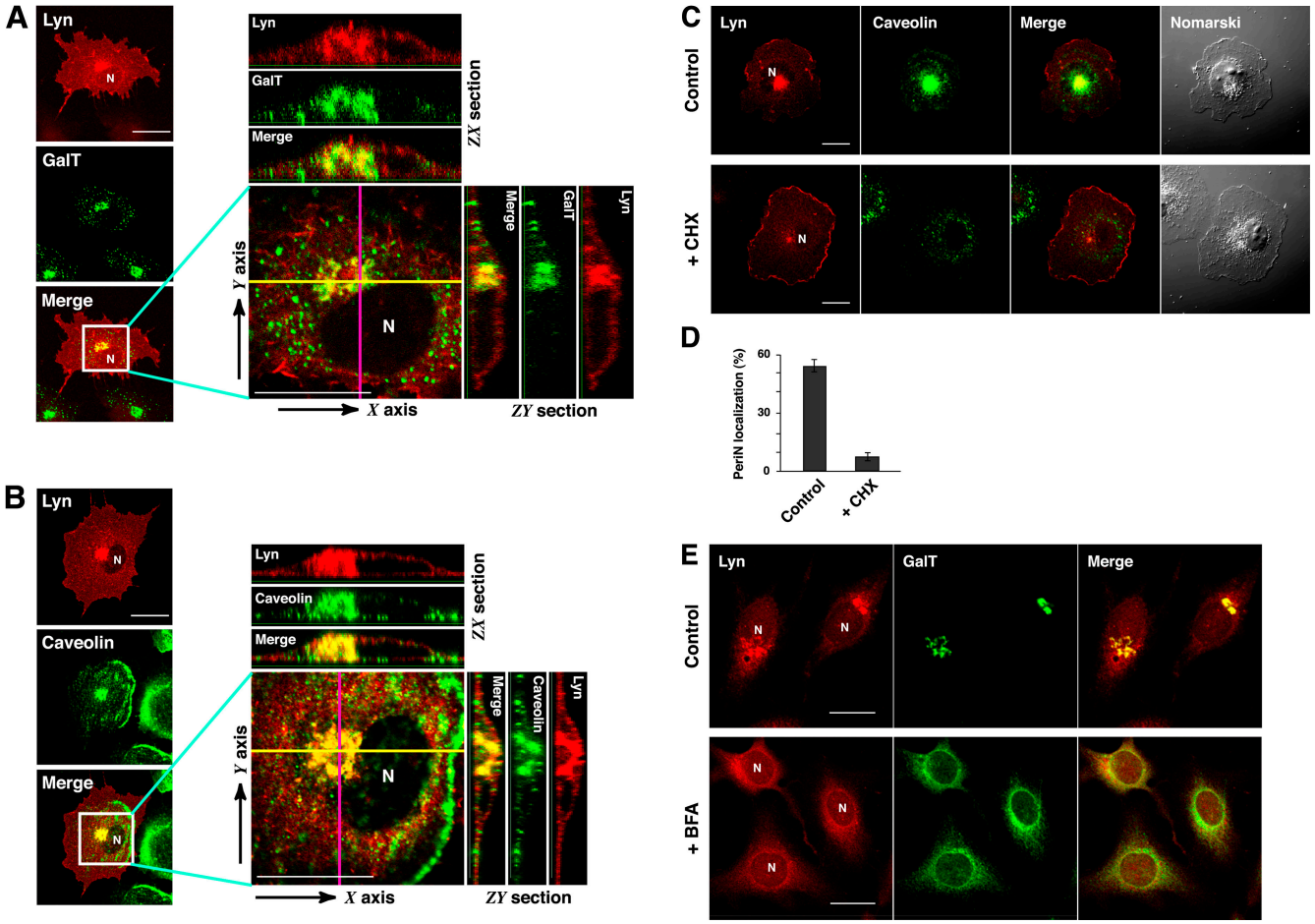

Figure 2. **Colocalization of Lyn with the Golgi pool of caveolin at the perinuclear region.** COS-1 cells were transfected with Lyn, and stained with anti-Lyn (red) in conjunction with (A) anti-galactosyltransferase (anti-GalT; green) or (B) anti-caveolin (green). All Z-series sections at 0.3–0.5-μm intervals were merged in two-dimensional xy images. Orthogonal sections viewing axial directions (xz and yz) are created in the margins. (C and D) COS-1 cells transfected with Lyn-HA were cultured for 18 h in the presence or absence of 200 μg/ml CHX during the last 3 h. Cells were double stained with anti-Lyn (red) and anti-caveolin (green). (D) Cells exhibiting the perinuclear localization of Lyn were quantified. Results (%) are the mean ± SD from three independent experiments. (E) HeLa cells were incubated in the absence (top) or presence (bottom) of 5 μg/ml BFA for 1 h. Cells were double stained with anti-Lyn (red) and anti-GalT (green). N, nucleus. Bars, 20 μm.

the kinase activity. We further identify four negative-charged amino acid residues, which are conserved among Src-family kinases and aligned on one side of the C-lobe of the kinase domain, responsible for the trafficking of Lyn to the plasma membrane. Our findings demonstrate the significance of the C-lobe through an open conformation for export of Lyn from the Golgi apparatus to the plasma membrane.

Results

Predominant localization of Lyn to the perinuclear region caused by kinase-domain deletion

To explore an element that can affect subcellular localization of Lyn, we examined the localization of a kinase-active Lyn mutant (Lyn-HA) and a kinase-domain deleted Lyn mutant (LynΔK-HA; Fig. 1 A) by generating HeLa cell clones that express Lyn-HA or LynΔK-HA in an inducible manner. When induced by addition of doxycycline, a tetracycline derivative, Lyn-HA was detected at the plasma membrane and the perinuclear region (Fig. 1 B), whereas LynΔK-HA was predominantly seen in the perinuclear region (Fig. 1 C). Until 3 h after induction, protein expression could not be detected by our immunostaining. In the course of induction, a majority of Lyn-HA was initially observed in the perinuclear region and subsequently detected at the plasma membrane (Fig. 1 D), whereas LynΔK-HA was almost restricted to the perinuclear region during the observation period (Fig. 1 E). These results suggest that upon expression Lyn may initially become accumulated at the perinuclear region, and that its subsequent appearance at the plasma membrane may involve the kinase domain.

Furthermore, transient expression of Lyn and its mutants in COS-1 cells enabled us to classify their features of localization as three patterns (PeriN, PeriN = PM, and PM) on the basis of ratios in amounts of expressed proteins between the perinuclear region (PeriN) and the plasma membrane (PM) (Fig. 1 F; see Materials and methods). Fig. 1 G shows that (a) Lyn, (b) Lyn-HA, and (c) LynΔK-HA irrespective of the difference in structure were predominantly observed in the perinuclear region during the earlier phase of expression. In the later phase, a majority of Lyn and Lyn-HA were observed at the plasma membrane, whereas an appreciable frac-

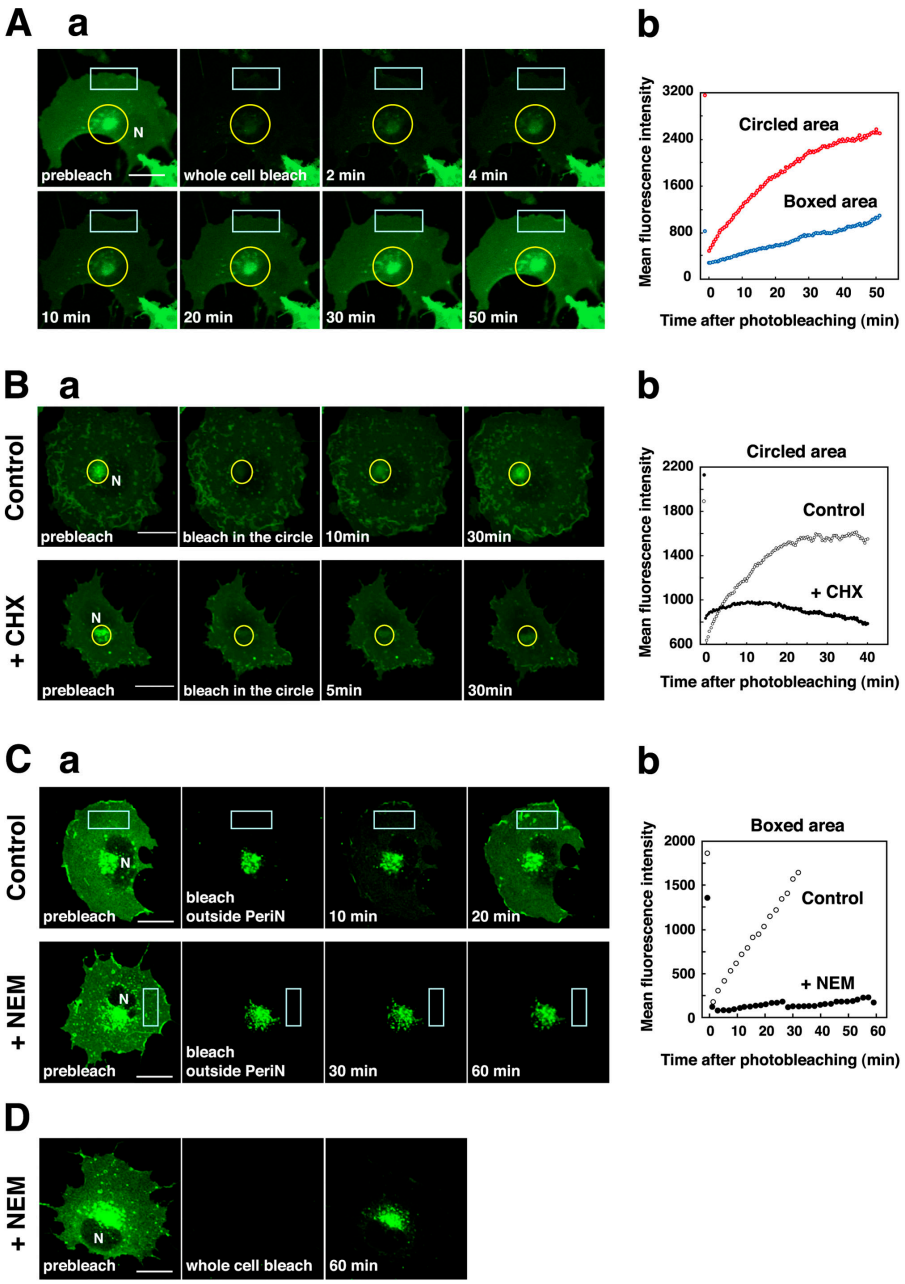

Figure 3. **Lyn trafficking through the Golgi pool of caveolin after biosynthesis.** Lyn trafficking was visualized in living COS-1 cells that were transfected with Lyn-GFP and cultured for 1 d. (A, a) Whole area of a cell was bleached, and the cell was monitored for the next 50 min at 20-s intervals. Times are shown from completion of the photobleaching. (b) Quantification of fluorescence recovery in the perinuclear region (circled area) and the plasma membrane (boxed area). Mean fluorescence intensities of recovery after photobleaching are plotted versus time. (B) (a) The perinuclear region (circled area) was bleached, and then the cell was monitored for the next 40 min at 20-s intervals in the absence or presence of 200 μg/ml CHX from 1 h before bleaching. (b) Quantification of fluorescence recovery in the perinuclear region (circled area). (C, a) Whole cell area excluding the perinuclear region was bleached, and then the cell was monitored for the next 30 or 60 min at 2-min intervals in the absence or presence of 300 μM NEM from 15 min before photobleaching. (b) Quantification of fluorescence recovery in the plasma membrane (boxed areas). (D) Whole cell area including the perinuclear region was bleached, and then the cell was cultured for 60 min in the presence of 300 μM NEM from 15 min before photobleaching. N, nucleus. Bars, 20 μm.

tion of LynΔK-HA still resided in the perinuclear region. These results are consistent with the results of HeLa cells shown in Fig. 1 (D and E).

Spatial association of Lyn with caveolin at the Golgi apparatus

To characterize the perinuclear region, cross sections of the confocal images were acquired in the z axis. Fig. 2 A shows that a large fraction of perinuclear Lyn was colocalized with β-1,4-galactosyltransferase (GalT), a trans-Golgi resident protein. Notably, Lyn was precisely colocalized with caveolin in the perinuclear region whereas Lyn and caveolin were poorly colocalized at the plasma membrane (Fig. 2 B). These results indicate that Lyn is colocalized with a pool of caveolin at the Golgi apparatus.

The recent data suggest that the presence of the Golgi pool of caveolin is dependent on new protein synthesis and not on exchange with caveolin at the plasma membrane or in endosomes (Nichols, 2002). To examine the relationship between Lyn and caveolin at the Golgi apparatus, cells were treated with cycloheximide (CHX), an inhibitor of protein synthesis. As shown in Fig. 2 (C and D), treatment of Lyn-expressing cells with CHX emptied caveolin from the Golgi apparatus, which was accompanied by elimination of perinuclear Lyn. However, CHX treatment did not disturb localization of Lyn to the plasma membrane. Given that Lyn and caveolin were poorly colocalized at the plasma membrane (Fig. 2 B), these results implicate that Lyn may be temporarily associated with caveolin at the Golgi apparatus before its reach to the plasma membrane.

Next, to examine whether localization of endogenous Lyn was similar to that of overexpressed Lyn, we immunostained HeLa and COS-1 cells with anti-Lyn. As shown in Fig. 2 E (top), endogenous Lyn was colocalized with

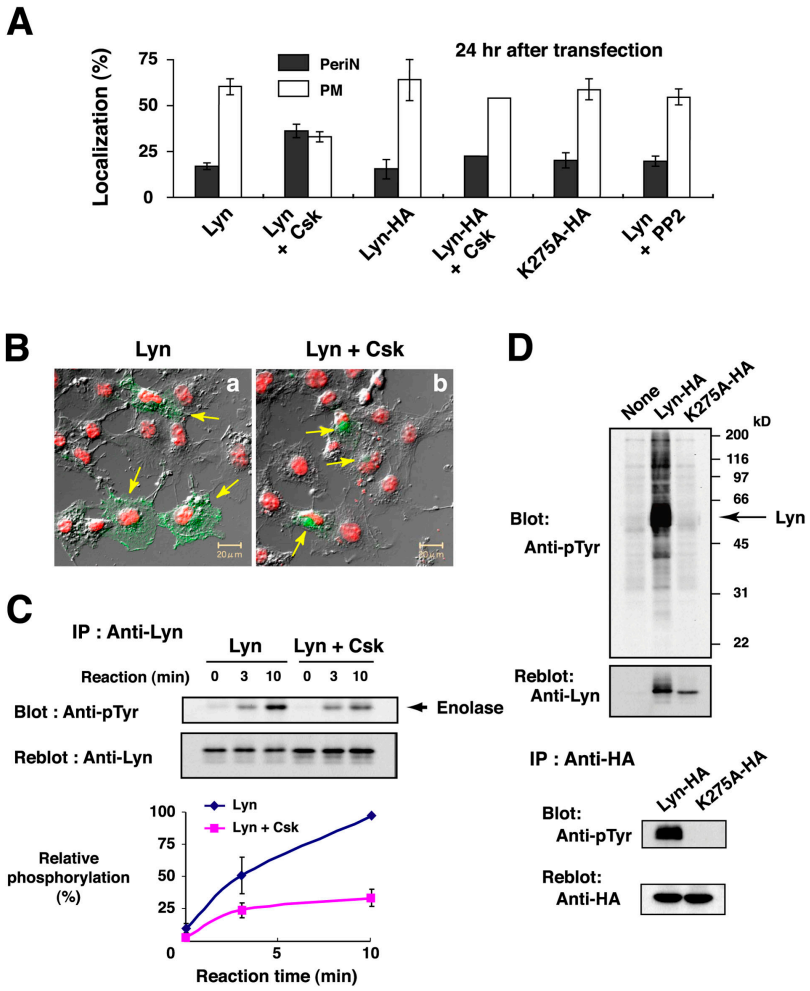

Figure 4. **Inhibition of Lyn trafficking by Csk, but not by Lyn inactivation.** (A) COS-1 cells transfected with Lyn, Lyn plus Csk, Lyn-HA, or Lyn(K275A)-HA were cultured for 24 h, and stained with anti-Lyn or anti-HA. COS-1 cells transfected with Lyn were cultured for 24 h, and treated with or without 10 μM PP2. Lyn localization was classified as described in Fig. 1 F. Results (%) are the mean ± SD from three independent experiments. COS-1 cells transfected with Lyn-HA plus Csk were cultured for 24 h. Results (%) of a representative experiment are shown for localization of Lyn-HA. PeriN, filled bars; PM, open bars. (B) COS-1 cells transfected with Lyn (a) or Lyn plus Csk (b) were cultured for 24 h, and stained with anti-Lyn. Arrows indicate cells expressing Lyn. Lyn, green; DNA, red. Bars, 20 μm. (C) Lyn immunoprecipitates prepared from COS-1 cells transfected with Lyn or Lyn plus Csk were subjected to in vitro kinase assays. Kinase reactions were determined by probing with anti-pTyr, and amounts of Lyn immunoprecipitates were analyzed by subsequent reprobing with anti-Lyn. The levels of tyrosine phosphorylation of enolase relative to the amounts of Lyn at each reaction time were quantified. Results are the mean ± SD from three independent kinase assays. (D) COS-1 cells were transfected with Lyn-HA or Lyn(K275A)-HA and cultured for 48 h. (Top) Western blot of equal amounts of Triton X-100 lysates was probed with anti-pTyr, and subsequently reprobed with anti-Lyn. The positions of size markers in kilodaltons are shown on the right. (Bottom) Immunoprecipitates of Lyn mutants with anti-HA were probed with anti-pTyr, and amounts of the immunoprecipitates were analyzed by subsequent reprobing with anti-HA.

GalT in HeLa cells as observed in Lyn-transfected COS-1 cells (Fig. 2 A). Although endogenous Lyn was detected in COS-1 cells by Western blotting, it could not be visualized by our immunostaining probably due to lower expression (unpublished data). We then tested the localization of endogenous Lyn for sensitivity to brefeldin A (BFA), because BFA is known to cause disassembly and redistribution of the Golgi apparatus into the ER (Klausner et al., 1992). Fig. 2 E (bottom) shows that endogenous Lyn present at the Golgi apparatus was dispersed by BFA treatment in accordance with redistribution of GalT into the ER. The dispersal of Lyn from the Golgi apparatus was also observed in Lyn-HA–expressing COS-1 cells (Fig. 7 A). These results suggest that both endogenous Lyn and overexpressed Lyn are similarly localized to the Golgi apparatus in a BFA-sensitive manner.

Trafficking of newly synthesized Lyn through the Golgi apparatus toward the plasma membrane

The Lyn-GFP fusion protein contains the almost entire structure of Lyn-HA, including the NH_2-terminal lipid attachment sites for myristoylation and palmitoylation, and is likely to preserve all functions of Lyn-HA. Indeed, the localization of Lyn-GFP visualized by fluorescence of GFP or anti-Lyn immunostaining was consistent with that of Lyn-HA detected by anti-Lyn or anti-HA immunostaining (unpublished data). Using FRAP techniques, the trafficking of Lyn-GFP after biosynthesis was monitored in living COS-1 cells transfected with Lyn-GFP. When whole cell area was photobleached, rapid recovery of Lyn-GFP fluorescence was observed in both the perinuclear region (Fig. 3 A, circled area) and the plasma membrane (Fig. 3 A, boxed area). In particular, the recovery rate of Lyn-GFP fluorescence in the perinuclear region was much higher than that at the plasma membrane. Upon expression of adequate levels of Lyn-GFP mRNA, FRAP can ensure rapid detection of trafficking of Lyn-GFP just after biosynthesis. The apparently slow kinetics (Fig. 1, D–G) could be explained by our inability to immunodetect Lyn proteins at low levels of Lyn mRNA during the early phase of induction.

When perinuclear Lyn-GFP was selectively photobleached, rapid recovery of Lyn-GFP fluorescence was observed in the perinuclear region (Fig. 3 B). In sharp contrast, treatment with CHX completely blocked recovery of perinuclear Lyn-GFP after the selective photobleaching of the perinuclear region. These results indicate that the appearance of Lyn at the Golgi apparatus requires protein biosynthesis, suggesting that Lyn barely recycles from the plasma membrane to the Golgi apparatus.

To test whether vesicular transport was required for localization of Lyn-GFP to the plasma membrane, we used *N*-ethyl-maleimide (NEM), a reagent known to block a wide

range of vesicular fusion events (Bivona et al., 2004). Fluorescence recovery of Lyn-GFP was monitored in the absence or presence of NEM after whole cell area excluding the perinuclear region was photobleached. As shown in Fig. 3 C, treatment of Lyn-GFP–expressing cells with NEM strongly blocked fluorescence recovery of Lyn-GFP at the plasma membrane (boxed area). Photobleaching of whole cell area in the presence of NEM ensured fluorescence recovery of Lyn-GFP at the perinuclear region (Fig. 3 D). These results suggest that newly synthesized Lyn is initially transported to the Golgi apparatus by nonvesicular transport but not targeted directly to the plasma membrane, and that the trafficking of Lyn from the Golgi apparatus en route to the plasma membrane is mediated by exocytic vesicular transport.

Requirement of the kinase domain but not kinase activity for Lyn trafficking to the plasma membrane

The catalytic activity of Src-family kinases is inhibited by creating a "closed conformation" through Csk tyrosine kinase-mediated phosphorylation of the COOH-terminal tyrosine residue (Brown and Cooper, 1996). To examine whether the kinase activity was required for localization of Lyn to the plasma membrane, we cotransfected COS-1 cells with Lyn and Csk. Their concomitant expression was found to increase the localization of Lyn to the Golgi apparatus and to decrease that to the plasma membrane (Fig. 4, A and B). In vitro kinase assays verified the inhibition of Lyn kinase activity by coexpressed Csk (Fig. 4 C). Localization of Lyn-HA, which is devoid of the COOH-terminal tyrosine residue, to the plasma membrane was unaffected by Csk coexpression (Fig. 4 A), indicating the inhibition through Csk-mediated phosphorylation of the COOH-terminal tyrosine residue of Lyn.

We then created a kinase-inactive mutant, Lyn(K275A)-HA by replacing Lys-275 to alanine in the ATP-binding site. Fig. 4 D confirmed that Lyn(K275A)-HA was deficient in tyrosine kinase activities for phosphorylation of cellular proteins and autophosphorylation. To our surprise, localization of Lyn(K275A)-HA was essentially similar to that of Lyn-HA (Fig. 4 A). Furthermore, treatment with PP2, a Src inhibitor that accesses a hydrophobic pocket-structure near the ATP-binding cleft of Src-family kinases (Zhu et al., 1999), was unable to inhibit localization of Lyn to the plasma membrane (Fig. 4 A), although the kinase activity of Lyn was greatly reduced (not depicted). These findings demonstrate that the kinase domain per se but not the kinase activity plays an important role in localization of Lyn to the plasma membrane.

The C-lobe responsible for Lyn trafficking to the plasma membrane

To identify a structure or an element in the kinase domain responsible for the localization, we constructed various deletion mutants of Lyn-HA and analyzed the expressed proteins in COS-1 cells by Western blotting. As shown in Fig. 5 A, each of these mutant proteins was detected at the expected size and the expression level of each protein was comparable. Fig. 5 B provides evidence that the localization of Lyn to the plasma membrane involves the structure encom-

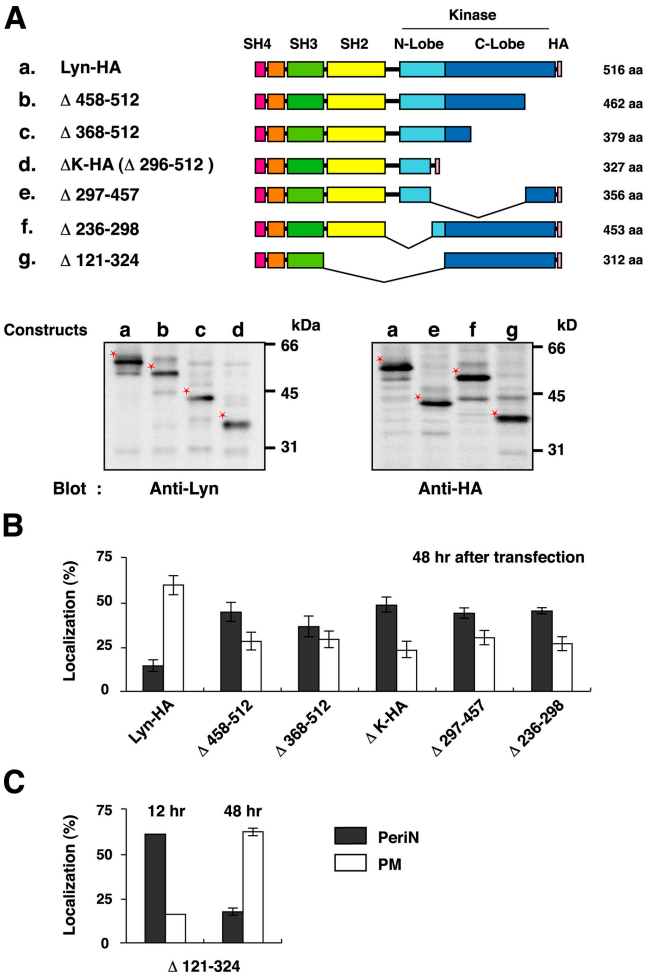

Figure 5. **Involvement of the COOH-terminal kinase lobe in Lyn trafficking.** (A) Schematic representations of Lyn-HA and its deletion mutants are shown. COS-1 cells were transfected with each of Lyn mutants, and cultured for 48 h. Western blots of equal amounts of Triton X-100 lysates were probed with anti-Lyn or anti-HA. Asterisks indicate the expressed proteins. (B) After transfection with each of Lyn mutants, COS-1 cells were cultured for 48 h. Results (%) of localization of Lyn mutants are the mean ± SD from three independent experiments, as described in Fig. 1 F. (C) Results (%) of localization of Δ 121-324 at 12 and 48 h after transfection into COS-1 cells are shown from a representative and three independent experiments, respectively. PeriN, filled bars; PM, open bars.

passing amino acids 236–506 in Lyn-HA, suggesting the importance of the NH_2- and COOH-terminal lobes of the kinase domain. However, the crystal structures of Hck and c-Src indicate that the αA helix in the SH2 domain electrostatically interacts with the αE and αI helices in the C-lobe of the kinase domain (Fig. 6 A; Xu et al., 1997; Sicheri et al., 1997). If electrostatic interactions between the SH2 domain and the C-lobe are extremely strengthened by deletion of both the SH2 linker and the N-lobe that might function as a spring hinge, one would predict that the SH2 domain tightly masks an element on the C-lobe responsible for plasma membrane localization. Therefore, we created the Lyn mutant (Δ 121-324) by deletion of the SH2 domain, the SH2 linker and the N-lobe (Fig. 5 A). Fig. 5 C reveals that, like Lyn-HA, the Lyn mutant (Δ 121-324) was initially

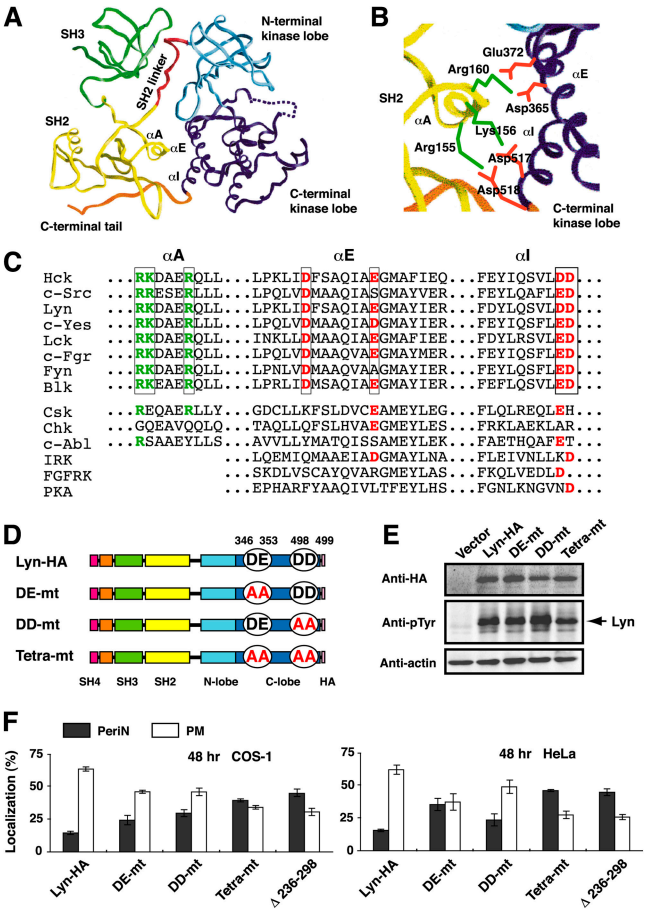

Figure 6. **Inhibition of Lyn trafficking by mutation of four charged amino acid residues.** (A) Src structure in the inactive state, represented by the SH3 (green) and SH2 (yellow) domains, the SH2 linker (red), the NH_2-terminal (light blue) and COOH-terminal (purple) kinase lobes, and the COOH-terminal tail (orange). (B) The interaction of the COOH-terminal kinase lobe and the SH2 domain via positively (green) and negatively (red) charged side chains in Hck. The figures (A and B) are modified from Sicheri et al. (1997) and Williams et al. (1998). (C) Amino acid sequence alignment of the Src family, the Csk family (Csk and Chk), c-Abl, insulin receptor kinase (IRK), fibroblast growth factor receptor kinase (FGFRK), and cAMP-dependent protein kinase (PKA). Positively and negatively charged residues are shown in green and red, respectively. (D) Schematic representations of Lyn-HA and its alanine-substitution mutants are shown. (E) COS-1 cells were transfected with Lyn mutants, and cultured for 48 h. Western blot of equal amounts of Triton X-100 lysates was probed with anti-pTyr, and subsequently reprobed with anti-HA and anti-actin. (F) COS-1 cells (left) or HeLa cells (right) were transfected with Lyn mutants, and cultured for 48 h. Results (%) of Lyn localization are the mean ± SD from three independent experiments, as described in Fig. 1 F. PeriN, filled bars; PM, open bars.

accumulated at the Golgi apparatus and was then able to efficiently localize to the plasma membrane. This indicates that the N-lobe is dispensable for the plasma membrane localization. It should be noted that the αE and αI helices are positioned side by side on the same surface of the C-lobe (Fig. 6 A). Therefore, it is likely that the αE and αI helices present on the C-lobe are candidate structures that could be only exposed to the molecular surface of Lyn in an "open conformation" but be masked in a "closed conformation" induced by Csk phosphorylation.

Identification of four negative-charged residues on the C-lobe

The overall organization of c-Src and Hck (Fig. 6 A) and the interaction of the SH2 and catalytic domains (Fig. 6 B) were provided (Sicheri et al., 1997; Xu et al., 1997; Williams et al., 1998). Structure-based amino acid sequence alignment indicates that three positive-charged residues on the αA helix in the SH2 domain and four negative-charged residues aligned on one side of the αE and αI helices in the C-lobe are conserved among members of the Src family (Fig. 6 C), predicting that Lyn, similar to c-Src and Hck, is structurally organized with the αA helix (Arg-136, Lys-137 and Arg-141) in the SH2 domain, and with the αE (Asp-346 and Glu-353) and αI (Asp-498 and Asp-499) helices in the C-lobe.

We created three alanine-substitution mutants of the C-lobe, DE-mt, DD-mt, and Tetra-mt, as depicted in Fig. 6 D. The levels of protein expression and kinase activity for autophosphorylation were comparable in COS-1 cells transfected with Lyn-HA or each Lyn mutant (Fig. 6 E). Intriguingly, mutations of the negative-charged residues were found to inhibit the localization of Lyn-HA to the plasma membrane in both COS-1 cells and HeLa cells (Fig. 6 F). Among DE-mt, DD-mt, and Tetra-mt, Tetra-mt exhibited the maximum inhibition of plasma membrane localization, which closely corresponded to the data of Lyn(Δ 236-298) as a control (Fig. 5 B, compare Δ 236-298 with ΔK-HA). These results suggest that the four negative-charged residues in the C-lobe play a role in the trafficking of Lyn-HA to the plasma membrane.

Role of four negative-charged residues in the C-lobe in the trafficking of Lyn

Next, we examined whether localization of Lyn-HA and Tetra-mt was affected by treatment with BFA. Fig. 7 B shows that Tetra-mt, like Lyn-HA (Fig. 7 A, top), was colocalized with GalT in the absence of BFA. The levels of Tetra-mt that were accumulated at the Golgi apparatus appeared to be slightly higher than those of Lyn-HA as judged by fluorescence intensities (Fig. 7, compare B with A). Upon treatment with BFA, Tetra-mt and Lyn-HA were both dispersed from the Golgi apparatus in the same way (Fig. 7, A and B, bottom). These results suggest that the association of Lyn with the Golgi apparatus may be unaffected by the mutation in the C-lobe.

To examine whether the four negative-charged residues in the C-lobe were involved in transport of Lyn from the Golgi apparatus to the plasma membrane and/or accumulation of Lyn at the Golgi apparatus, we constructed the GFP-tagged version of Tetra-mt (Tetra-mt-GFP) by replacing Asp-346, Glu-353, Asp-498, and Asp-499 present in the C-lobe of Lyn-GFP with four alanines. The pattern of localization of Tetra-mt-GFP to the Golgi apparatus was indistinguishable from that of Tetra-mt (unpublished data; Fig. 6 F). Then, we compared the trafficking of Lyn-GFP with that of Tetra-mt-GFP. Using FRAP, fluorescence recovery of Lyn-GFP or Tetra-mt-GFP was simultaneously monitored in both the perinuclear region (Fig. 7, C and D, circled area) and the plasma membrane (Fig. 7, C and D, boxed area) after whole

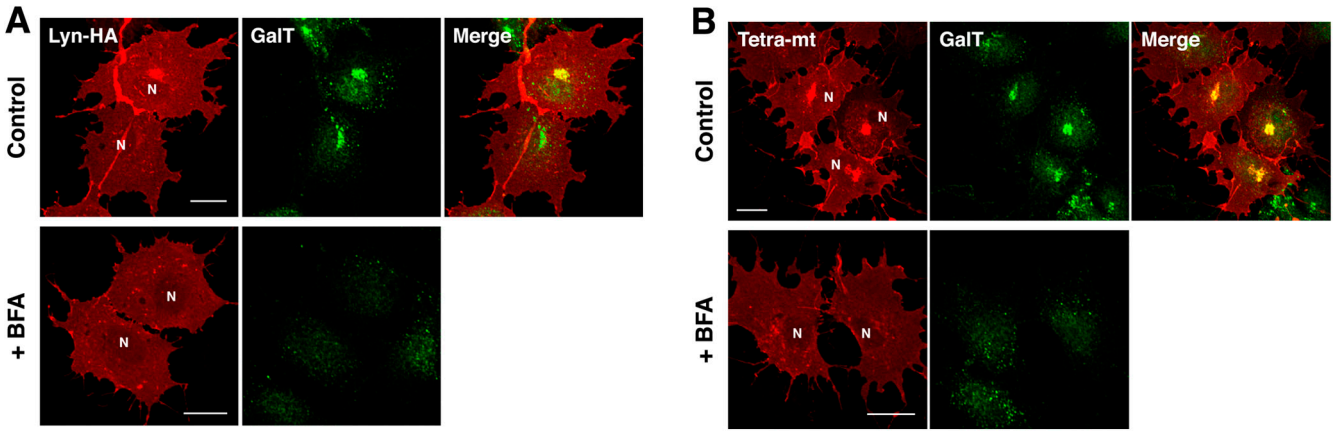

Figure 7. **Involvement of the four charged residues in transport of Lyn from the Golgi to the plasma membrane.** COS-1 cells transfected with Lyn-HA (A) or Tetra-mt (B) were cultured for 1 d in the absence or presence of 5 μg/ml BFA during the last 1 h. Cells were double stained with anti-Lyn (red) and anti-GalT (green). (C and D) Lyn trafficking was visualized in living COS-1 cells transfected with Lyn-GFP (C) or Tetra-mt-GFP (D). (a) Whole area of a cell was bleached, and the cell was monitored for the next 90–110 min at 2-min intervals. Times are shown from completion after the photobleaching. (b) Quantification of fluorescence recovery in the perinuclear region (circled area) and the plasma membrane (boxed area). Mean fluorescence intensities of recovery after photobleaching are plotted versus time. N, nucleus. Bars, 20 μm.

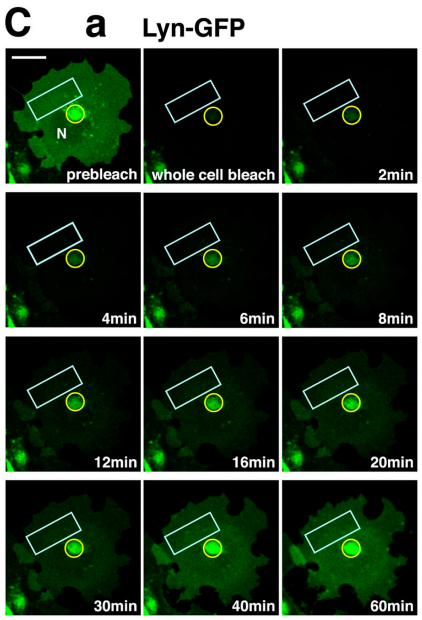

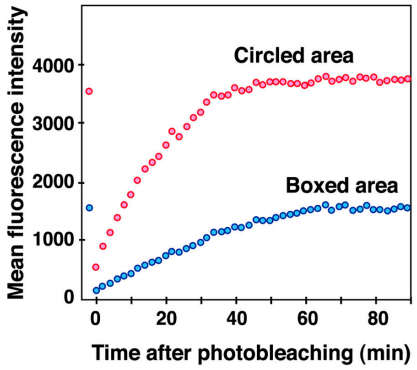

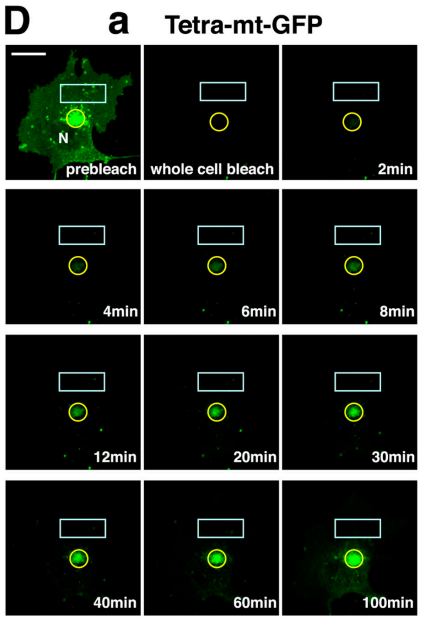

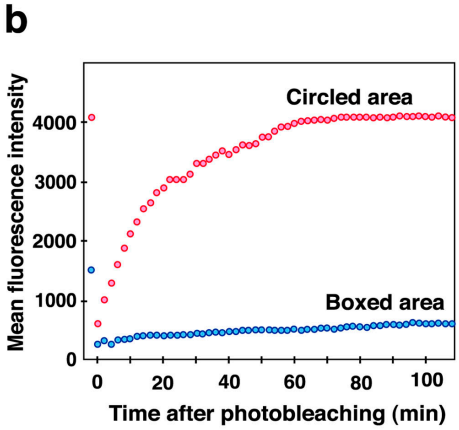

cell area was photobleached. Fig. 7 C shows that rapid recovery of Lyn-GFP fluorescence was observed in the perinuclear region (circled area). This rapid response was similar to that of fluorescence recovery of Tetra-mt-GFP in the perinuclear region (Fig. 7 D, circled area). The plateau levels in fluorescence recovery were also comparable between Lyn-GFP and Tetra-mt-GFP (Fig. 7, C and D, circled area). In sharp contrast to the perinuclear region, the rate of fluorescence recovery of Tetra-mt-GFP at the plasma membrane (Fig. 7 D, boxed area) greatly decreased as compared with that of Lyn-GFP at the plasma membrane (Fig. 7 C, boxed area). These results suggest that the mutation of the four charged residues is unlikely to affect the association of Lyn at the Golgi apparatus just after biosynthesis. Rather, the mutation markedly impeded the trafficking of Lyn from the Golgi apparatus toward the plasma membrane. These results implicate that the four negative-charged residues on the C-lobe may be involved in an export process of Lyn from the Golgi apparatus.

Discussion

Here, we demonstrate that the kinase domain of Lyn plays a significant role in Lyn trafficking besides catalysis of substrate phosphorylation. By using FRAP and immunostaining for pursuing spatial and temporal localization of Lyn, we show that newly synthesized Lyn is accumulated at the Golgi pool of caveolin and then transported to the plasma membrane in a kinase domain-dependent but kinase activity-independent manner. Furthermore, we have identified four negative-charged amino acid residues in the C-lobe of the kinase domain as being important for transport of Lyn from the Golgi apparatus toward the plasma membrane.

It is well known that nonreceptor-type tyrosine kinases contain modular domains for protein–protein interactions, such as the SH2 and SH3 domains (Pawson, 1995). In the repressed state, the SH2 and SH3 domains of Src-family kinases and of Abl tyrosine kinase can confer their autoinhibited "closed conformation" through intramolecular interactions (Sicheri et al., 1997; Xu et al., 1997; Hantschel et al., 2003; Nagar et al., 2003). In the activated state, these modular domains exposed by an "open conformation" can interact with adaptor or substrate proteins, thereby transmitting signals downstream. It should be noted that the trafficking of Lyn can be inhibited by Csk-mediated phosphorylation of the COOH-terminal tyrosine residue of Lyn (Fig. 4, A–C). Nonetheless, the trafficking of the kinase-inactive Lyn mutant obviously proceeds to the plasma membrane (Fig. 4). Therefore, we assume a novel Csk-induced mechanism for inhibition of Lyn trafficking, independently of the kinase-activity inhibition, which could not be explained by the well-established autoinhibition mechanism (Brown and Cooper, 1996; Gonfloni et al., 1999; Hubbard, 1999; Xu et al., 1999). Mutational analyses further reveal that the four negative-charged amino acid residues of the C-lobe in the kinase domain, which may be exposed to the molecular surface in an "open conformation" (Fig. 6 A), is involved in the trafficking of Lyn from the Golgi apparatus to the plasma membrane (Fig. 6 F and Fig. 7). Accordingly, we hypothesize that an "open conformation" of Lyn unmasks the αE and αI helices within the C-lobe of the kinase domain including the four negative-charged amino acid residues that may function for the proper trafficking through potential protein–protein interactions.

Treatment with BFA disperses the Golgi localization of Lyn, accompanied by disassembly of the Golgi apparatus (Fig. 2 E; Fig. 7, A and B), suggesting that the transport of Lyn to the plasma membrane may share membrane transport via the Golgi apparatus in the secretory pathway. The observations of whole cell bleaching in FRAP experiments indicate that the localization of Lyn to the Golgi apparatus appears to precede plasma membrane localization (Fig. 3 A). Furthermore, inhibition of protein synthesis shows that the localization of Lyn at the Golgi apparatus actually requires protein synthesis (Fig. 3 B), suggesting that Lyn already transported to the plasma membrane does not move back from the plasma membrane to the Golgi apparatus. Intriguingly, the export of Lyn from the Golgi apparatus to the plasma membrane is specifically inhibited by treatment with NEM (Fig. 3, C and D), further indicating that the transport is assisted with membrane vesicles of the exocytic pathway. The C-lobe of the kinase domain is involved in export of Lyn from the Golgi apparatus to the plasma membrane (Figs. 6 and 7), whereas the SH4, unique, SH3 and SH2 domains are not (Fig. 5). Together, we can imagine that localization of Lyn to the Golgi apparatus is prerequisite for its trafficking to the plasma membrane along the exocytic vesicular transport pathway, i.e., one-way or vectorial trafficking of Lyn through the Golgi apparatus. Perhaps the C-lobe may actively participate in and accelerate an export process on the cytoplasmic side of vesicles at the Golgi apparatus, because Lyn must be anchored on the outer surface of membrane vesicles through lipid modification. Alternatively, given that accumulation of newly synthesized Lyn at the Golgi apparatus can reach a plateau at similar rates and levels irrespective of the mutation of four negative-charged residues on the C-lobe (Fig. 7, C and D), Lyn might be protected from proteolytic degradation in the Golgi milieu due to the negative-charged residues on the C-lobe. Further studies will decipher a precise role of the C-lobe in Lyn trafficking.

Caveolins form lipid-raft platforms of a variety of signaling molecules at the plasma membrane and are important for transporting cholesterol and glycosylphosphatidylinositol-linked proteins (Liu et al., 2002). Caveolins are also involved in endocytic and exocytic transport (Scheiffele et al., 1998; Pelkmans et al., 2001; Nichols, 2002). Caveolin-containing endosomes are implicated as sites for the sorting of caveolin away from the Golgi-bound cargos (Nichols, 2002). Our cross sections of the confocal images demonstrate that Lyn colocalizes with caveolin at the Golgi apparatus (Fig. 2, A and B). It is of substantial interest to note that minimal colocalization of Lyn with caveolin is detected at the plasma membrane despite flawless colocalization of Lyn with caveolin at the Golgi apparatus (Fig. 2, B and C). Although a role of caveolin in Lyn trafficking is still unclear, Lyn may be dissociated from caveolin-containing vesicles during transport of Lyn from the Golgi apparatus en route to the plasma membrane.

Mutation of the COOH-terminal tyrosine residue or deletion of the kinase domain of c-Src was reported to dramat-

ically redistribute c-Src from perinuclear endosomal membranes to focal adhesions (Kaplan et al., 1994), suggesting that the SH2 and SH3 domains of c-Src in an "open conformation" can be exposed for association with focal adhesions. However, despite the presence of the SH4, unique, SH3 and SH2 domains, the localization of the kinase domain-deleted Lyn (LynΔK-HA) to the perinuclear region (Fig. 1) is quite different from that of the kinase domain-deleted c-Src to focal adhesions. Even though the COOH-terminal negative tyrosine residue of Lyn is mutated for formation of an activated "open conformation," the pattern of localization of Lyn-HA is dissimilar to that of the corresponding mutant of c-Src (Fig. 1; for review see Kaplan et al., 1994). Thus far, it has been reported that c-Src, Lck, Fyn, Hck, and c-Yes are enriched in the perinuclear region (Resh and Erikson, 1985; David-Pfeuty and Nouvian-Dooghe, 1990; Kaplan et al., 1992; Ley et al., 1994; Gauen et al., 1996; Bijlmakers et al., 1997; Carreno et al., 2000; McCabe and Berthiaume, 2001). In our view emerged from literature surveys, the localizations of Lck and Hck to the perinuclear region seem to be similar to the restricted localization of Lyn shown in this work, whereas c-Src and c-Yes appear to be more widely distributed around the nucleus. In fact, we observed minimal colocalization of c-Src with caveolin in the perinuclear region and no elimination of c-Src from the perinuclear region by inhibition of protein synthesis (Fig. 2, C and D; unpublished data). These results raise the intriguing possibility that two close relatives, Lyn and c-Src, localize to at least two different subcellular organelles in the perinuclear region, i.e., the Golgi pool of caveolin and caveolin-negative endosomes, for their presumable distinct functions.

Why does newly synthesized Lyn initially localize and accumulate at the Golgi apparatus? Recent evidence provides a novel view that endomembranes, such as the Golgi apparatus and the ER, may serve as a platform of signaling molecules. For example, Ras that is restricted to the endomembranes can activate the Erk pathway in response to mitogenic stimulation and play a role in transformation of fibroblasts (Chiu et al., 2002). It is also observed that phosphatidylinositol-3,4,5-trisphosphate levels are increased to a larger extent at the endomembranes than at the plasma membrane, which is triggered by endocytosed receptor tyrosine kinases (Sato et al., 2003). Therefore, it would be tempting to assume that accumulation of Lyn at the Golgi apparatus is important in unidentified signal transduction at endomembranes. Alternatively, previous studies with T cells suggested that Lck can associate with the cytoplasmic domain of the cell surface transmembrane protein CD4 at the Golgi apparatus early after synthesis or long before CD4 has reached the plasma membrane (Bijlmakers et al., 1997; Bijlmakers and Marsh, 1999). In addition, dual myristoylation and palmitoylation are needed for membrane association, because myristoylated proteins are either soluble or only weakly associated with membranes (Resh, 1999) after the covalent attachment of myristic acid to an NH_2-terminal glycine at the amino acid position 2 occurs cotranslationally in the cytoplasm (Wilcox et al., 1987). Another possibility may be addressed that a site of palmitoylation of Lyn might be located in the Golgi apparatus because a species of palmitoyl acyltransferase is hypothesized to reside at the Golgi apparatus (Bijlmakers and Marsh, 2003). Although these possibilities are mutually inclusive, further studies will be required to understand a key role for localization of Lyn to the Golgi apparatus besides the plasma membrane.

It is clear from this work that transport of Lyn to the plasma membrane is far more complex than initially thought. It should be emphasized that a structure of the kinase domain per se plays a novel role for Lyn trafficking. At present, it is particularly interesting to determine how an "open conformation" of the kinase domain operates during protein trafficking. In addition, the mechanisms of trafficking should be compared between Lyn and c-Src for further understanding of different localizations of these Src-family kinases.

Materials and methods

Plasmid constructs

Lyn lacking the kinase domain (LynΔK, 1-298; the number referring to the amino acid position from the initiator methionine) was constructed (Hirao et al., 1998) from human wild-type p56 Lyn cDNA (Yamanashi et al., 1987; provided by T. Yamamoto, University of Tokyo, Tokyo, Japan). LynΔK was ligated into the pMH vector (Roche), resulting in the HA-tagged version (LynΔK-HA). The HA-tagged kinase-active Lyn (Lyn-HA) was designed to replace the COOH-terminal negative regulatory region (507-512 containing Tyr508) with the HA epitope by PCR using the sense primer 5′-AGATGAGCTCTATGACATTATGAA-3′ and the antisense primer 5′-TTTCTAGAGTCTAAGCGTAGTCTGGGACGTCGTATGGGTA-ACCTTCCGTGGCTGTGTAGAAA-3′. The Lys→Ala mutation at position 275 in the ATP-binding site (kinase-inactive, K275A) was generated by site-directed mutagenesis according to the protocol (Stratagene) with Lyn-HA as a template using the sense primer 5′-CTATAACAACAGTACTAAGGTGGCT-GTGGCAACCCTGAAGCCAGG-3′ and the antisense primer 5′-CCTG-GCTTCAGGGTTGCCACAGCCACCTTAGTACTGTTGTTATAG-3′. DE-mt (Asp346→Ala, Glu353→Ala) and DD-mt (Asp498→Ala, Asp499→Ala) were created using Lyn-HA as a template with the respective primer combinations: the sense primer 5′-CAAAGCTCATTGCCTTTTCTGCGCAGATTG-CAGCGGGAATGGCATAC-3′ and the antisense primer 5′-GTATGCCAT-TCCCGCTGCAATCTGCGCAGAAAAGGCAAGAGCTTTG-3′; or the sense primer 5′-GACTACTTACAGAGCGTGCTAGCTGCTTTCTACACAGCCA-CGG-3′ and the antisense primer 5′-CCGTGGCTGTGTAGAAAGCAG-CTAGCACGCTCTGTAAGTAGTC-3′. Tetra-mt (Asp346→Ala, Glu353→Ala, Asp498→Ala, Asp499→Ala) was constructed from DE-mt and DD-mt. Δ 458-512 (1-457), Δ 368-512 (1-367), Δ 297-457 (1-296 and 458-506), Δ 236-298 (1-235 and 299-506), and Δ 121-324 (1-120 and 325-506) were generated from Lyn-HA using appropriate restriction enzymes and blunting. The resulting fragments were all confirmed by sequencing. Lyn-GFP and Tetra-mt-GFP was constructed by fusion with GFP obtained from pEGFP-C1 (CLONTECH Laboratories, Inc.) at the COOH terminus of Lyn-HA and Tetra-mt, respectively. The constructs were subcloned into the pMKITneo vector (provided by K. Maruyama, Tokyo Medical and Dental University, Tokyo, Japan) or the tetracycline-inducible pcDNA4/TO vector (Invitrogen). Rat Csk cDNA (Nada et al., 1991; provided by M. Okada and S. Nada, Osaka University, Osaka, Japan), tagged with the HA-epitope at the COOH terminus into the pMH vector (Csk-HA, 1-440), was ligated into the pCAG vector (Niwa et al., 1991; provided by J. Miyazaki, Osaka University).

Antibodies

Monoclonal anti-HA (F-7; Santa Cruz Biotechnology, Inc., and 3F10; Roche), anti-Lyn (H-6; Santa Cruz Biotechnology, Inc.), antiphosphotyrosine (anti-pTyr; 4G10; Upstate Biotechnology), and anti-actin (MAB1501; CHEMICON International, Inc.) were used. Affinity-purified rabbit anti-GalT (Yamaguchi and Fukuda, 1995; provided by M.N. Fukuda, The Burnham Institute, La Jolla, CA), anti-Lyn (H-44; Santa Cruz Biotechnology, Inc.), and anti-caveolin (Transduction) were used. HRP-$F(ab')_2$ of antibodies to mouse, rat, or rabbit Ig were purchased from Amersham Biosciences. FITC-$F(ab')_2$ of anti–rabbit IgG or of anti–mouse IgG and TRITC-anti–mouse IgG were obtained from Biosource International and Sigma-Aldrich.

Cells and transfection

COS-1 cells and HeLa cells (Japanese Collection of Research Bioresources) were cultured in Iscove's modified DME containing 5% FBS. T-REx™-

HeLa cells (Invitrogen) that express the tetracycline repressor were maintained in Iscove's modified DME containing 5% FBS and 0.2 μg/ml blasticidin, and cells were transfected with the pcDNA4/TO vector (Invitrogen) encoding LynΔK-HA or Lyn-HA using the TransIT Transfection reagent (Mirus; Yamaguchi et al., 2001), and cell clones were selected in 250 μg/ml Zeocin (Invitrogen) plus 0.2 μg/ml blasticidin. Doxycycline, a derivative of tetracycline, was used for protein expression. COS-1 and HeLa cells were transiently transfected with 0.2 μg or 1.0 μg of plasmid vectors using TransIT. For inhibition of Lyn kinase activity, COS-1 cells transfected with Lyn were cultured for 6 h, and treated with PP2 (Calbiochem; Hanke et al., 1996) for the next 18 h.

Immunofluorescence and photobleaching experiments

Cells were fixed with 4% PFA, permeabilized with 0.1% saponin, and mounted with ProLong antifade reagent (Molecular Probes) after immunostaining (Tada et al., 1999; Yamaguchi et al., 2001). Confocal and Nomarski differential-interference-contrast images were obtained using an LSM510 (Carl Zeiss MicroImaging, Inc.) or Fluoview FV500 (Olympus) laser scanning microscope with a 20× 0.50 NA or a 40× 0.75 NA objective, or a 40× 1.00 NA oil or a 100× 1.35 NA oil immersion objective. Care was taken to ensure that detection sensitivity was kept constant and that there was no bleed-through from the fluorescein signal into the red channel (Yamaguchi et al., 2001). One planar (xy) section slice was shown in most experiments. Orthogonal sections viewing axial directions (xz and yz) were created when all Z-series sections at 0.25–0.5-μm intervals were merged. 100–800 cells were scored for each assay according to whether expressed proteins were highly restricted in the perinuclear region or at the plasma membrane. Results (%) were expressed as ratios of number of cells exhibiting these classified localizations to total number of cells expressing Lyn proteins. For FRAP experiments, COS-1 cells were transfected with Lyn-GFP or Tetra-mt-GFP, and cultured for 1 d. Cells were maintained above 30°C in a warmed room throughout photobleaching experiments that were performed on a stage of a Fluoview FV500 laser scanning microscope using the 488 nm line of an argon laser with a 40× 1.00 NA oil immersion objective to achieve sufficient depth for bleaching z. The circled area or whole area was photobleached at full laser power (100% power) and recovery of fluorescence was monitored by scanning the whole cell at low laser power (3.0% power). Time-lapse sequences were recorded with Fluoview Tiempo and the mean fluorescence intensities within regions of interest were quantified using Fluoview Tiempo time course version 4.2 software. Composite figures were prepared using Photoshop 5.0 and Illustrator 9.0 software (Adobe).

Western blotting, immunoprecipitation, and in vitro kinase assay

Lysates were prepared in Triton X-100 lysis buffer (50 mM Hepes, pH 7.4, 10% glycerol, 1% Triton X-100, 4 mM EDTA, 100 mM NaF, and 1 mM Na_3VO_4) containing 50 μg/ml aprotinin, 100 μg/ml leupeptin, 25 μM pepstatin A, and 2 mM PMSF. Immunoprecipitation was performed using anti-Lyn– or anti-HA–precoated protein-G beads. Immunodetection was performed as reported previously (Hirao et al., 1997; Mera et al., 2002). In vitro kinase assays were performed as described previously (Iwama et al., 1996; Hirao et al., 1997; Mera et al., 1999; Yamaguchi et al., 2001). In brief, Lyn was immunoprecipitated with anti-Lyn from Triton X-100 lysates of COS-1 cells transfected with Lyn or Lyn plus Csk. After washing, equal amounts of each immunoprecipitate were reacted with acid-denatured enolase in kinase buffer (50 mM Hepes, pH 7.4, 1% Triton X-100, 10 mM $MnCl_2$, 1 mM Na_3VO_4) containing 100 μM unlabeled ATP at 30°C for the indicated periods. Phosphorylated bands were immunodetected by anti-pTyr, and quantified with the Image Gauge software using an Image Analyzer LAS-1000plus (Fujifilm). Composite figures were prepared using Photoshop 5.0 and Illustrator 9.0 software (Adobe).

We are grateful to Drs. T. Yamamoto, M. Okada, S. Nada, M.N. Fukuda, K. Maruyama, and J. Miyazaki for plasmids and antibodies and T. Okumura for technical help.

This work was supported in part by grants-in-aid for Scientific Research from the Japanese Ministry of Education, Culture, Sports, Science and Technology.

Submitted: 1 March 2004
Accepted: 19 April 2004

References

Bijlmakers, M.J.E., and M. Marsh. 1999. Trafficking of an acylated cytosolic protein: newly synthesized $p56^{lck}$ travels to the plasma membrane via the exocytic pathway. *J. Cell Biol.* 145:457–468.

Bijlmakers, M.J.E., and M. Marsh. 2003. The on-off story of protein palmitoylation. *Trends Cell Biol.* 13:32–42.

Bijlmakers, M.J.E., M. Isobe-Nakamura, L.J. Ruddock, and M. Marsh. 1997. Intrinsic signals in the unique domain target $p56^{lck}$ to the plasma membrane independently of CD4. *J. Cell Biol.* 137:1029–1040.

Bivona, T.G., H.H. Wiener, I.M. Ahearn, J. Silletti, V.K. Chiu, and M.R. Philips. 2004. Rap1 up-regulation and activation on plasma membrane regulates T cell adhesion. *J. Cell Biol.* 164:461–470.

Blume-Jensen, P., and T. Hunter. 2001. Oncogenic kinase signaling. *Nature.* 411: 355–365.

Brown, M.T., and J.A. Cooper. 1996. Regulation, substrates and functions of src. *Biochim. Biophys. Acta.* 1287:121–149.

Carreno, S., M.E. Gouze, S. Schaak, L.J. Emorine, and I. Maridonneau-Parini. 2000. Lack of palmitoylation redirects $p59^{Hck}$ from the plasma membrane to $p61^{Hck}$-positive lysosomes. *J. Biol. Chem.* 275:36223–36229.

Chiu, V.K., T. Bivona, A. Hach, J.B. Sajous, J. Silletti, H. Wiener, R.L. Johnson II, A.D. Cox, and M.R. Phillips. 2002. Ras signalling on the endoplasmic reticulum and the Golgi. *Nat. Cell Biol.* 4:343–350.

David-Pfeuty, T., and Y. Nouvian-Dooghe. 1990. Immunolocalization of the cellular src protein in interphase and mitotic NIH c-src overexpresser cells. *J. Cell Biol.* 111:3097–3116.

Dykstra, M.L., A. Cherukuri, and S.K. Pierce. 2001. Floating the raft hypothesis for immune receptors: access to rafts controls receptor signaling and trafficking. *Traffic.* 2:160–166.

Gauen, J.K.T., M.E. Linder, and A.S. Shaw. 1996. Multiple features of $p59^{fyn}$ src homology 4 domain define a motif for immune-receptor tyrosine-based activation motif (ITAM) binding and for plasma membrane localization. *J. Cell Biol.* 133:1007–1015.

Gonfloni, S., F. Frischknecht, M. Way, and G. Superti-Furga. 1999. Leucine 255 of Src couples intramolecular interactions to inhibition of catalysis. *Nat. Struct. Biol.* 6:760–764.

Hanke, J.H., J.P. Gardner, R.L. Dow, P.S. Changelian, W.H. Brissette, E.J. Weringer, B.A. Pollok, and P.A. Connelly. 1996. Discovery of a novel, potent, and Src family-selective tyrosine kinase inhibitor. *J. Biol. Chem.* 271:695–701.

Hantschel, O., B. Nagar, S. Guettler, J. Kretzschmar, K. Dorey, J. Kuriyan, and G. Superti-Furga. 2003. A myristoyl/phosphotyrosine switch regulates c-Abl. *Cell.* 112:845–857.

Hayashi, T., H. Umemori, M. Mishina, and T. Yamamoto. 1999. The AMPA receptor interacts with and signals through the protein tyrosine kinase Lyn. *Nature.* 397:72–76.

Healy, J.I., and C.C. Goodnow. 1998. Positive versus negative signaling by lymphocyte antigen receptors. *Annu. Rev. Immunol.* 16:645–670.

Hirao, A., I. Hamaguchi, T. Suda, and N. Yamaguchi. 1997. Translocation of the Csk homologous kinase (Chk/Hyl) controls activity of CD36-anchored Lyn tyrosine kinase in thrombin-stimulated platelets. *EMBO J.* 16:2342–2351.

Hirao, A., X.L. Huang, T. Suda, and N. Yamaguchi. 1998. Overexpression of C-terminal Src kinase homologous kinase suppresses activation of Lyn tyrosine kinase required for VLA5-mediated Dami cell spreading. *J. Biol. Chem.* 273:10004–10010.

Hubbard, S.R. 1999. Src autoinhibition: let us count the ways. *Nat. Struct. Biol.* 6:711–714.

Iwama, A., N. Yamaguchi, and T. Suda. 1996. STK/RON receptor tyrosine kinase mediates both apoptotic and growth signals via the multifunctional docking sites conserved among the HGF receptor family. *EMBO J.* 15:5866–5875.

Kaplan, K.B., J.R. Swedlow, H.E. Varmus, and D.O. Morgan. 1992. Association of $pp60^{c\text{-}src}$ with endosomal membranes in mammalian fibroblasts. *J. Cell Biol.* 118:321–333.

Kaplan, K.B., K.B. Bibbins, J.R. Swedlow, M. Arnaud, D.O. Morgan, and H.E. Varmus. 1994. Association of the amino-terminal half of c-Src with focal adhesions alters their properties and its regulated by phosphorylation of tyrosine 527. *EMBO J.* 13:4745–4756.

Korade-Mirnics, Z., and S.J. Corey. 2000. Src kinase-mediated signaling in leukocytes. *J. Leukoc. Biol.* 68:603–613.

Klausner, R.D., J.G. Donaldson, and J. Lippincott-Schwartz. 1992. Brefeldin A: insights into the control of membrane traffic and organelle structure. *J. Cell Biol.* 116:1071–1080.

Ley, S.C., M. Marsh, C.R. Bebbington, K. Proudfoot, and P. Jordan. 1994. Distinct intracellular localization of Lck and Fyn protein tyrosine kinases in human T lymphocytes. *J. Cell Biol.* 125:639–649.

Linstedt, A.D., M.L. Vetter, J.M. Bioshop, and R.B. Kelly. 1992. Specific associa-

tion of the proto-oncogene product pp60$^{c\text{-}src}$ with an intracellular organelle, the PC12 synaptic vesicle. *J. Cell Biol.* 117:1077–1084.

Liu, P., M. Rudick, and R.G. Anderson. 2002. Multiple functions of caveolin-1. *J. Biol. Chem.* 277:41295–41298.

McCabe, J.B., and L.G. Berthiaume. 2001. N-terminal protein acylation confers localization to cholesterol, sphingolipid-enriched membranes but not to lipid rafts/caveolae. *Mol. Biol. Cell.* 12:3601–3617.

Mera, A., M. Suga, M. Ando, T. Suda, and N. Yamaguchi. 1999. Induction of cell shape changes through activation of the interleukin-3 common β chain receptor by the RON receptor-type tyrosine kinase. *J. Biol. Chem.* 274:15766–15774.

Mera, A., M. Suga, Y. Nakayama, M. Ando, T. Suda, and N. Yamaguchi. 2002. Redistribution of ERK/MAP kinase to uropod-like structures in interleukin-3-induced cell shape changes. *Immunol. Lett.* 84:117–124.

Mohn, H., V. LeCabec, S. Fischer, and I. Maridonneau-Parini. 1995. The src-family protein-tyrosine kinase p59^{hck} is located on the secretory granules in human neutrophils and translocates towards the phagosome during cell activation. *Biochem. J.* 309:657–665.

Nada, S., M. Okada, A. MacAuley, J.A. Cooper, and H. Nakagawa. 1991. Cloning of a complementary DNA for a protein-tyrosine kinase that specifically phosphorylates a negative regulatory site of p60$^{c\text{-}src}$. *Nature.* 351:69–71.

Nagar, B., O. Hantschel, M.A. Young, K. Scheffzek, D. Veach, W. Bornmann, B. Clarkson, G. Superti-Furga, and J. Kuriyan. 2003. Structural basis for the autoinhibition of c-Abl tyrosine kinase. *Cell.* 112:859–871.

Nichols, B.J. 2002. A distinct class of endosome mediates clathrin-independent endocytosis to the Golgi complex. *Nat. Cell Biol.* 4:374–378.

Niwa, H., K. Yamamura, and J. Miyazaki. 1991. Efficient selection for high-expression transfectants with a novel eukaryotic vector. *Gene.* 108:193–200.

Pawson, T. 1995. Protein modules and signalling networks. *Nature.* 373:573–580.

Pelkmans, L., J. Kartenbeck, and A. Helenius. 2001. Caveolar endocytosis of simian virus 40 reveals a new two-step vesicular-transport pathway to the ER. *Nat. Cell Biol.* 3:473–483.

Radha, V., S. Nambirajan, and G. Swarup. 1996. Association of Lyn tyrosine kinase with the nuclear matrix and cell-cycle-dependent changes in matrix-associated tyrosine kinase activity. *Eur. J. Biochem.* 236:352–359.

Resh, M.D. 1994. Myristylation and palmitylation of Src family members: the fats of the matter. *Cell.* 76:411–413.

Resh, M.D. 1999. Fatty acylation of proteins: new insights into membrane targeting of myristoylated and palmitoylated proteins. *Biochim. Biophys. Acta.* 1451:1–16.

Resh, M.D., and R.L. Erikson. 1985. Highly specific antibody to Rous sarcoma virus src gene product recognizes a novel population of pp60$^{v\text{-}src}$ and pp60$^{c\text{-}src}$ molecules. *J. Cell Biol.* 100:409–417.

Sato, M., Y. Ueda, T. Takagi, and Y. Umezawa. 2003. Production of $PtdInsP_3$ at endomembranes is triggered by receptor endocytosis. *Nat. Cell Biol.* 5:1016–1022.

Scheiffele, P., P. Verkade, A.M. Fra, H. Virta, K. Simons, and E. Ikonen. 1998. Caveolin-1 and -2 in the exocytic pathway of MDCK cells. *J. Cell Biol.* 140:795–806.

Sicheri, F., I. Moarefi, and J. Kuriyan. 1997. Crystal structure of the Src family tyrosine kinase Hck. *Nature.* 385:602–609.

Tada, J., M. Omine, T. Suda, and N. Yamaguchi. 1999. A common signaling pathway via Syk and Lyn tyrosine kinases generated from capping of the sialomucins CD34 and CD43 in immature hematopoietic cells. *Blood.* 93:3723–3735.

Thomas, S.M., and J.S. Brugge. 1997. Cellular functions regulated by Src family kinases. *Annu. Rev. Cell Dev. Biol.* 13:513–609.

Tsukita, S., K. Oishi, T. Akiyama, Y. Yamanashi, T. Yamamoto, and S. Tsukita. 1991. Specific proto-oncogenic tyrosine kinases of src family are enriched in cell-to-cell adherens junctions where the level of tyrosine phosphorylation is elevated. *J. Cell Biol.* 113:867–879.

van't Hof, W., and M.D. Resh. 1997. Rapid plasma membrane anchoring of newly synthesized p59fyn: selective requirement for NH_2-terminal myristoylation and palmitoylation at cysteine-3. *J. Cell Biol.* 136:1023–1035.

Wilcox, C., J.S. Hu, and E.N. Olson. 1987. Acylation of proteins with myristic acid occurs cotranslationally. *Science.* 238:1275–1278.

Williams, J.C., R.K. Wierenga, and M. Saraste. 1998. Insights into Src kinase functions:structural comparisons. *Trends Biochem. Sci.* 23:179–184.

Xu, W., S.C. Harrison, and M.J. Eck. 1997. Three-dimensional structure of the tyrosine kinase c-Src. *Nature.* 385:595–602.

Xu, W., A. Doshi, M. Lei, M.J. Eck, and S.C. Harrison. 1999. Features of its autoinhibitory mechanism. *Mol. Cell.* 3:629–638.

Yamaguchi, N., and M.N. Fukuda. 1995. Golgi retention mechanism of β-1,4-galactosyltransferase:membrane-spanning domain-dependent homodimerization and association with α- and β-tubulins. *J. Biol. Chem.* 270:12170–12176.

Yamaguchi, N., Y. Nakayama, T. Urakami, S. Suzuki, T. Nakamura, T. Suda, and N. Oku. 2001. Overexpression of the Csk homologous kinase (Chk tyrosine kinase) induces multinucleation: a possible role for chromosome-associated Chk in chromosome dynamics. *J. Cell Sci.* 114:1631–1641.

Yamanashi, Y., S. Fukushige, K. Semba, J. Sukegawa, N. Miyajima, K. Matsubara, T. Yamamoto, and K. Toyoshima. 1987. The *yes*-related cellular gene *lyn* encodes a possible tyrosine kinase similar to p56^{lck}. *Mol. Cell. Biol.* 7:237–243.

Zhu, X., J.L. Kim, J.R. Newcomb, P.E. Rose, D.R. Stover, L.M. Toledo, H. Zhao, and K.A. Morgenstern. 1999. Structural analysis of the lymphocyte-specific kinase Lck in complex with non-selective and Src family selective kinase inhibitors. *Structure.* 7:651–661.